

Transonic Aeroelastic Analysis of the X-59 Aircraft Using FUN3D

Walter A. Silva* Mark D. Sanetrik† Wesley W. Li‡ Shun-fat Lung§
Benjamin C. Park¶

The Low-Boom Flight Demonstrator (LBFD), or X-59 aircraft, was designed and fabricated by the Lockheed-Martin (LM) Corporation under a contract from NASA as part of the QueSST Mission. One of the primary goals is to demonstrate that a low sonic boom is achievable via aerodynamic shaping. The aircraft successfully completed its first flight, marking the beginning of an extensive envelope expansion campaign. In continued preparation for first flight and flight envelope expansion, the combined NASA/LM X-59 team prepared several documents towards Airworthiness Certification including various tests and analyses. Given that the aircraft will reach a maximum Mach number of 1.4, a transonic aeroelastic analysis has been generated to address any potential concerns. Three different methods, all based on the FUN3D code, were used to generate these solutions: FUN3D, FUN3D/AEROM, FUN3D/Linearized Frequency Domain (LFD). Results are presented for four Mach numbers: $M=0.95$, 0.97 , 0.99 , and 1.05 .

I. Introduction

The Low-Boom Flight Demonstrator (LBFD) aircraft, also known as the X-59, was designed and fabricated by the Lockheed-Martin Company under a NASA contract as part of NASA's QueSST Mission. The primary goal of the QueSST Mission is to acquire flight test data demonstrating an achievable low boom over land in order to effect change of current supersonic flight regulations. The X-59 aircraft has been designed with a shape to significantly reduce the sonic boom signature. There are three phases to the QueSST Mission: Phase 1 consisting of design, fabrication and envelope expansion; Phase 2 consisting of sonic boom signature data acquisition from X-59 flights over land from a limited number of airfields; and Phase 3 consisting of sonic boom data acquisition from X-59 flights over residential areas near major airports.

The X-59 is currently in Phase 1 of the project. With design and fabrication complete, the project successfully achieved first flight and is now progressing towards envelope expansion flights. In order to address potential concerns regarding aeroelastic stability at transonic Mach number conditions, CFD-based analyses were performed.

II. Low-Boom Flight Demonstrator, X-59

An image of the Low-Boom Flight Demonstrator (LBFD), or X-59, is presented in Figure 1. The X-59 has been designed and fabricated by the Lockheed-Martin Corporation under a contract from NASA in partial fulfillment of NASA's QueSST mission. The full paper will include structural details of the X-59 including results of structural tests performed to date.

*NASA Emeritus Langley Associate, Aeroelasticity Branch, AIAA Fellow.

†NASA Senior Research Engineer, Aeroelasticity Branch, AIAA Senior Member.

‡NASA Senior Research Engineer, Structures Branch, AIAA Senior Member.

§Retired, NASA Senior Research Engineer, Retired, AIAA Senior Member.

¶Retired, NASA Aerospace Engineer, Retired, AIAA Senior Member.



Figure 1. X-59 aircraft

III. Computational Methods

III.A. FUN3D Code

FUN3D is a CFD software suite developed at NASA Langley Research Center.¹ The primary solver is a node-centered finite volume discretization.² For aeroelastic simulations, FUN3D uses a linear elasticity analogy to deform the volume mesh and modal solver to represent the structure.³ The mode shapes from the finite element model are projected onto the aerodynamic surface with radial basis function interpolation. For time-domain aeroelastic simulations, dual time stepping is used to converge the governing equations at each time step of the backwards difference formulation scheme.

Recent work in FUN3D added a Streamline Upwind Petrov-Galerkin (SUPG) stabilized finite-element solver (FUN3D/SFE)⁴ and a corresponding Linearized Frequency Domain (LFD) solver.⁵ The LFD method linearizes the SUPG governing equations about some nonlinear equilibrium solution, either a steady jig shape or static aeroelastic solution, then solves the flow response to a harmonic perturbation input in the frequency domain. For a flutter analysis, the harmonic perturbations are the mesh motion due to movement of the mode shapes, and the frequency-domain Generalized Aerodynamic Forces (GAFs) are computed as the inner product of the linearized forces from the flow response to the harmonic input and the mode shapes. An independent LFD linear system is solved for the combination of modes being perturbed and a set of frequencies that cover the range of expected flutter frequencies. The resulting set of GAFs are then fed into a flutter (p-k, k, g-method) solver to compute the aeroelastic response.

For both the time-domain finite volume solutions and the LFD simulations, Spalart Allmaras (SA) turbulence model is utilized.⁶ For FUN3D/SFE and LFD simulations, the negative variant of SA (SA-neg)⁷ is applied.

III.B. AEROM

In structural dynamics, the realization of discrete-time state-space models that describe the modal dynamics of a structure has been enabled by the development of algorithms such as the Eigensystem Realization Algorithm (ERA)⁸ and the Observer Kalman Identification (OKID)⁹ Algorithm. These algorithms perform state-space realizations by using the Markov parameters (discrete-time impulse responses) of the systems

of interest. These algorithms have been combined into one package known as SOCIT developed at NASA Langley Research Center.

There are several algorithms within the SOCIT that are used for the development of unsteady aerodynamic discrete-time state-space models. The PULSE algorithm is used to extract individual input/output impulse responses from simultaneous input/output responses. For a four-input/four-output system, simultaneous excitation of all four inputs yields four output responses. The PULSE algorithm is used to extract the individual sixteen (all combinations of four inputs and four outputs) impulse responses that associate the response in each of the outputs due to each of the inputs. Once the individual sixteen impulse responses are available, they are then processed via the ERA in order to transform the sixteen individual impulse responses into a four-input/four-output, discrete-time, state-space model. A brief summary of the basis of this algorithm follows.

A finite dimensional, discrete-time, linear, time-invariant dynamical system has the state-variable equations

$$x(k+1) = Ax(k) + Bu(k) \quad (1)$$

$$y(k) = Cx(k) + Du(k) \quad (2)$$

where x is an n -dimensional state vector, u an m -dimensional control input, and y a p -dimensional output or measurement vector with k being the discrete time index. The transition matrix, A , characterizes the dynamics of the system. The goal of system realization is to generate constant matrices (A , B , C , D) such that the output responses of a given system due to a particular set of inputs is reproduced by the discrete-time state-space system described above.

For the system of Eqs. (1) and (2), the time-domain values of the discrete-time impulse responses of the system are also known as the Markov parameters and are defined as

$$Y(k) = CA^{k-1}B + D \quad (3)$$

with A an ($n \times n$) matrix, B an ($n \times m$) matrix, C a ($p \times n$) matrix, and D an ($p \times m$) matrix. The ERA algorithm begins by defining the generalized Hankel matrix consisting of the discrete-time impulse responses for all input/output combinations. The algorithm then uses the singular value decomposition to compute the (A , B , C , D) matrices.

In this fashion, the ERA is applied to unsteady aerodynamic impulse responses to construct unsteady aerodynamic state-space models. The AEROM software includes the necessary SOCIT routines as well as additional routines to manage the data flow and model generation.

III.B.1. AEROM Development Processes

The application of AEROM for the development of an aeroelastic ROM consists of two parts: the creation of the unsteady aerodynamic ROM and the creation of the structural dynamic ROM. The combination of the unsteady aerodynamic ROM with the structural dynamic ROM yields what is referred to as the aeroelastic simulation ROM.

An outline of the AEROM development process is as follows:

1. Generate the number of functions (from a selected family of orthogonal functions) that corresponds to the number of structural modes;
2. Apply the generated input functions simultaneously via one CFD execution resulting in GAF responses due to these inputs; these responses are computed directly from the restart of a steady rigid CFD solution (not about a particular dynamic pressure);
3. Using the simultaneous input/output responses, identify the individual impulse responses using the PULSE algorithm (within SOCIT);
4. Transform the individual impulse responses generated in Step 3 into an unsteady aerodynamic state-space system using the ERA (within SOCIT);
5. Evaluate/validate the state-space models generated in Step 4 via comparison with CFD results (i.e., ROM results vs. full CFD solution results);

A schematic of steps 1-4 of the AEROM process outlined above is presented as Figure 2.

Using modal information (generalized masses, modal frequencies, and modal dampings), a state-space model of the structure is generated. This state-space model of the structure is referred to as the structural dynamic ROM (see Figure 3). Once an unsteady aerodynamic ROM and a structural dynamic ROM have been generated, they are combined to form an aeroelastic simulation ROM (see Figure 4). Then root locus plots are extracted from the aeroelastic simulation ROM.

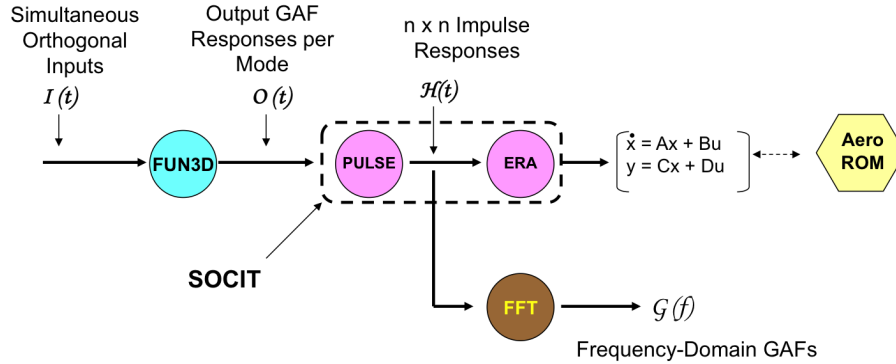


Figure 2. Improved process for generation of an unsteady aerodynamic ROM (Steps 1-4).

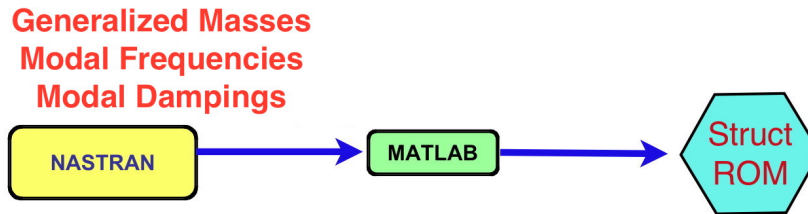


Figure 3. Process for generation of a structural dynamic state-space ROM.

Details of the AEROM software are available in the References.¹⁰

IV. Sample Results

A sample set of results to be included in the full paper is presented in this section. The full paper will include results from time-domain FUN3D solutions, AEROM solutions, and LFD solutions at several transonic Mach numbers. Results for linear aeroelastic analyses using the ZAERO code will be presented as well.

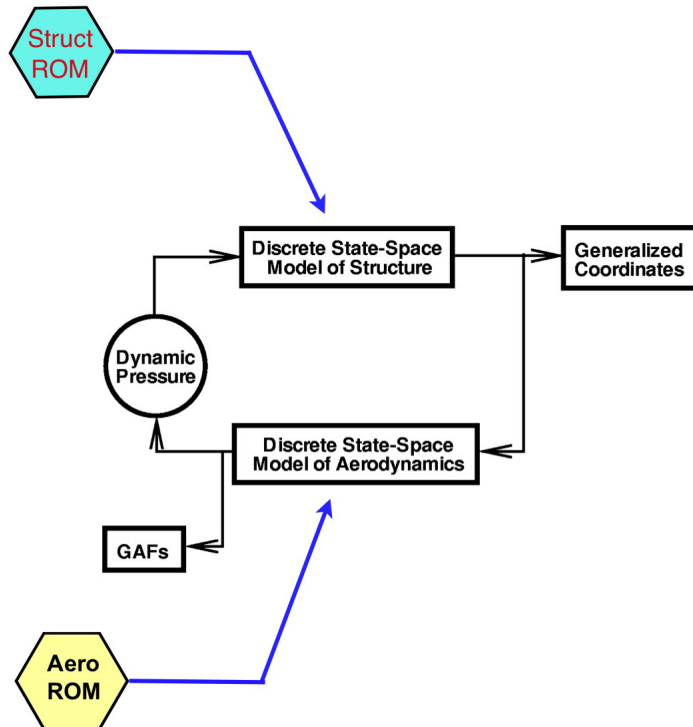


Figure 4. Process for generation of an aeroelastic simulation ROM consisting of an unsteady aerodynamic ROM and a structural state-space ROM.

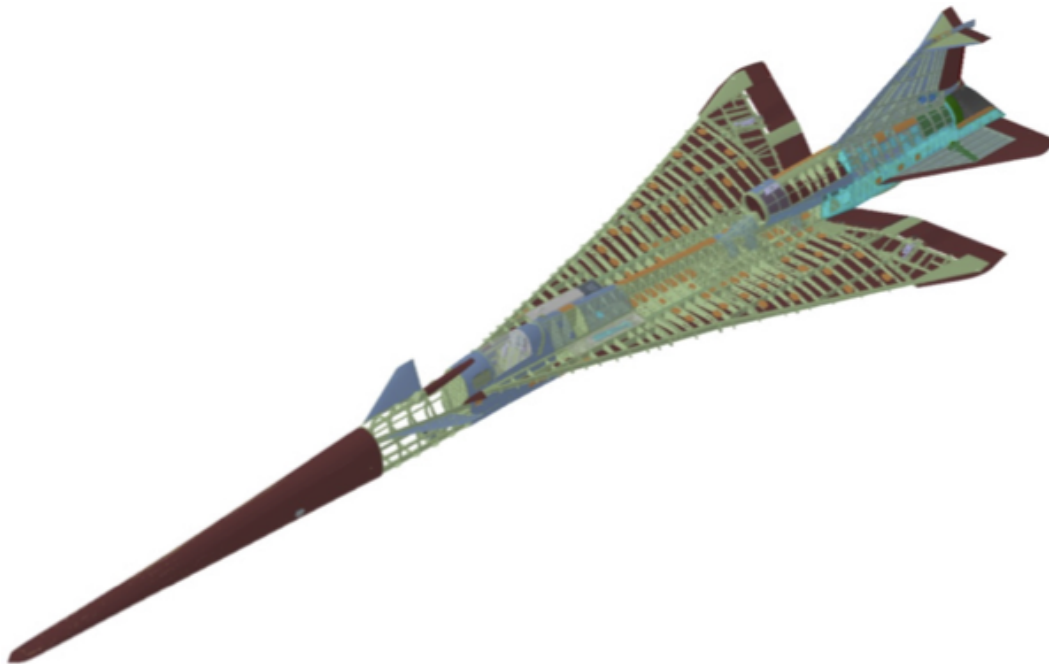


Figure 5. Finite element model (FEM).

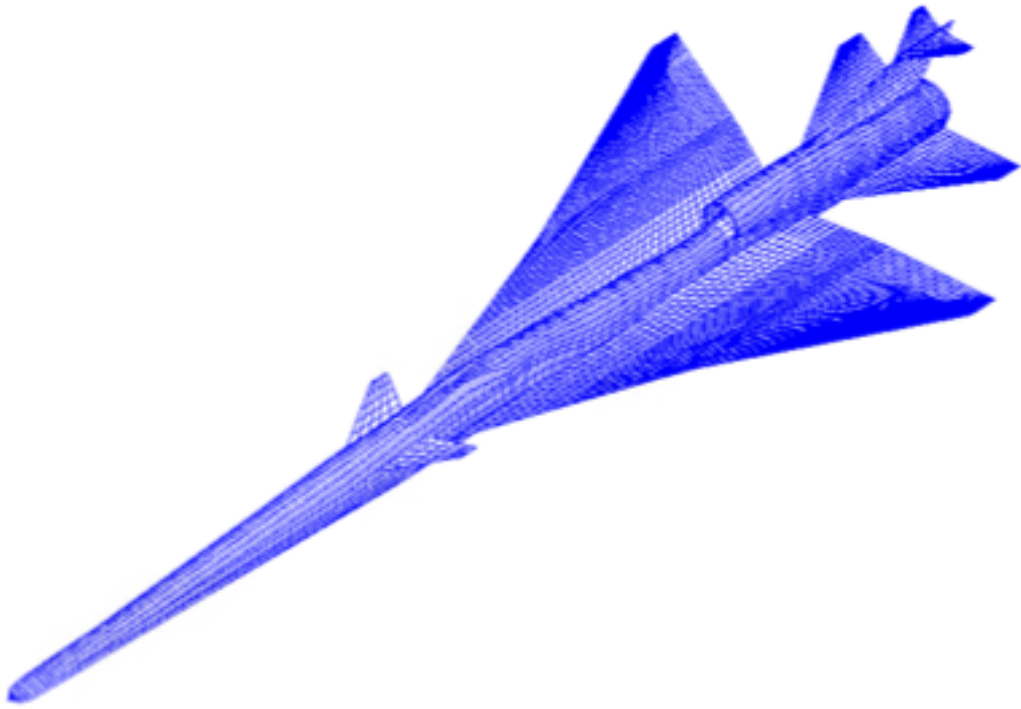


Figure 6. The ZAERO code aerodynamic panel layout.

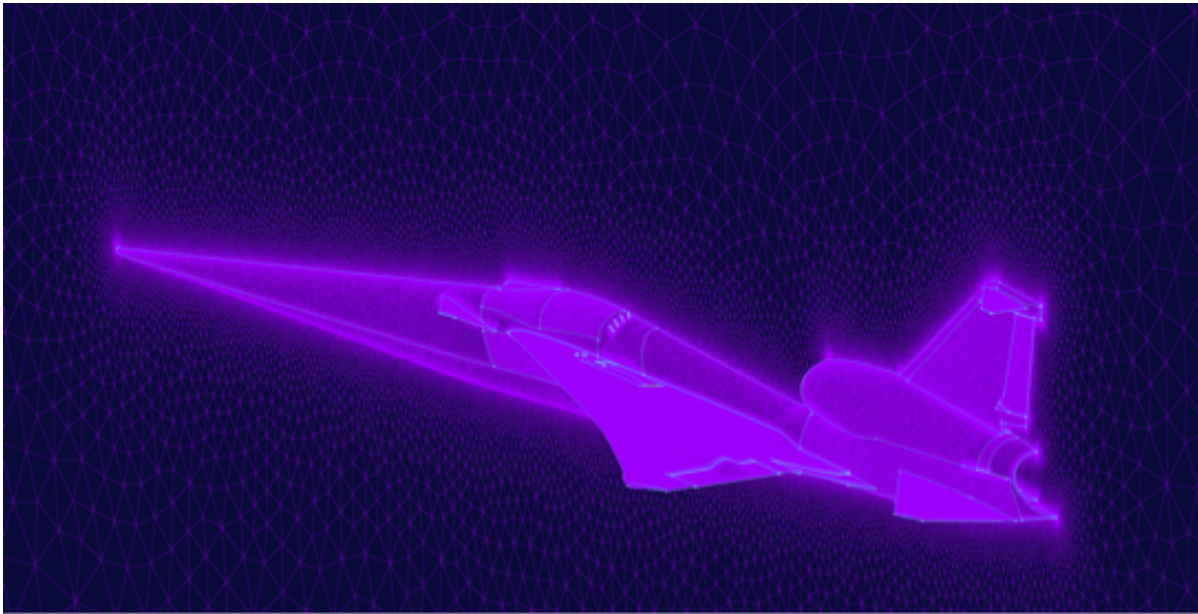


Figure 7. Unstructured grid consisting of 31 million grid points.

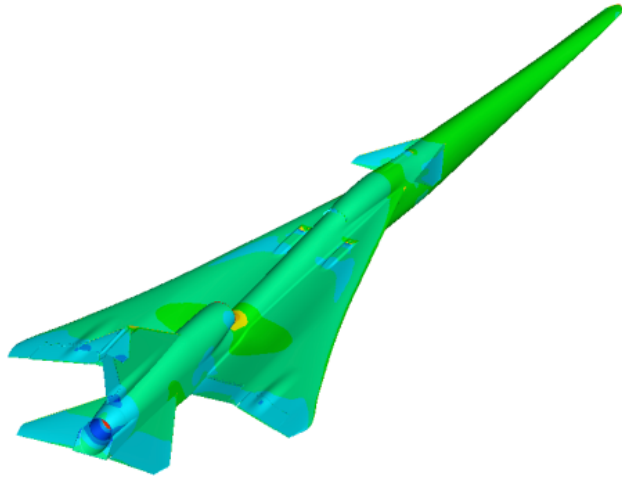


Figure 8. Pressure coefficient contour plot for $M=1.05$.

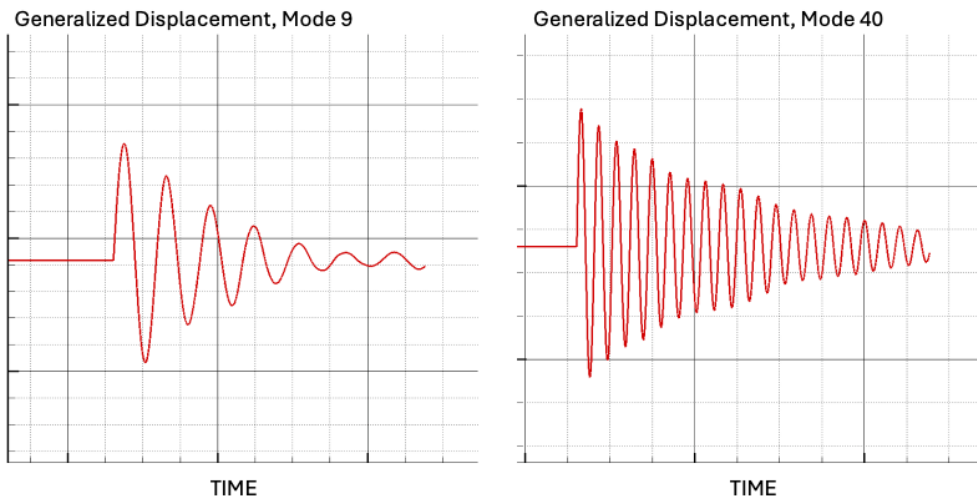


Figure 9. FUN3D aeroelastic generalized coordinates for $M=0.95$ at $Q=216$ psf for flexible modes 9 and 40.

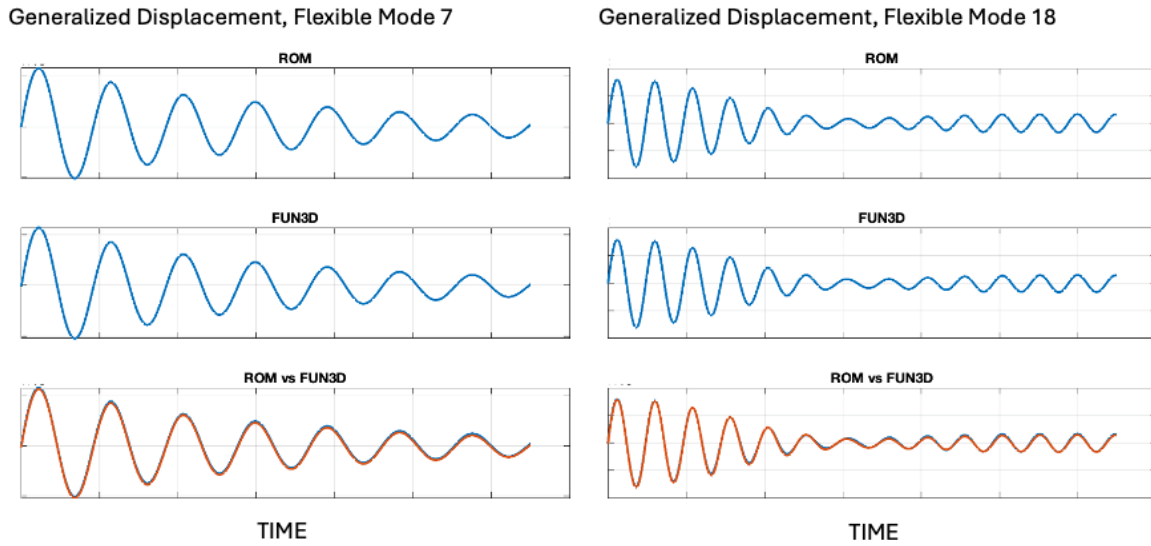


Figure 10. Comparison of AEROM and FUN3D aeroelastic generalized coordinates for $M=0.99$ at $Q=216$ psf for flexible modes 7 and 18.

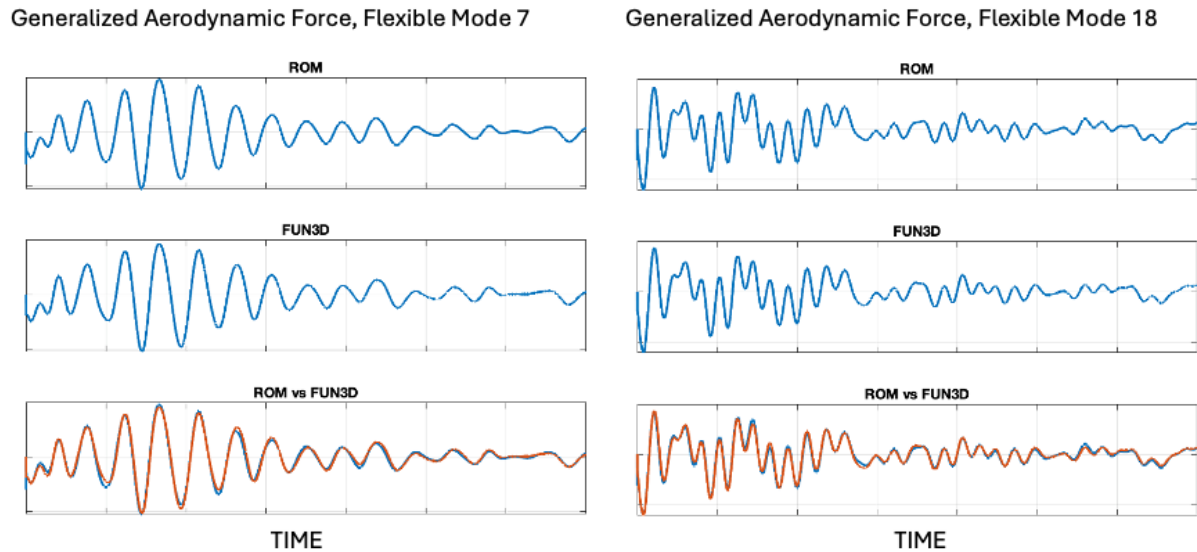
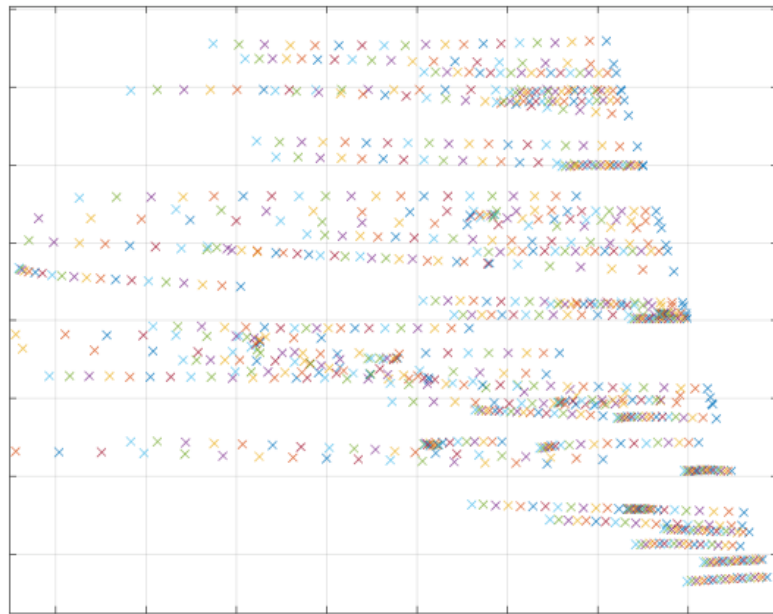


Figure 11. Comparison of AEROM and FUN3D aeroelastic generalized aerodynamic forces for $M=0.99$ at $Q=216$ psf for flexible modes 7 and 18.

Imaginary



Real

Figure 12. AEROM-generated aeroelastic root locus plot for $M=0.99$, from $Q=0$ to $Q=432$ psf, for 49 flexible modes including GVT-measured structural damping values.

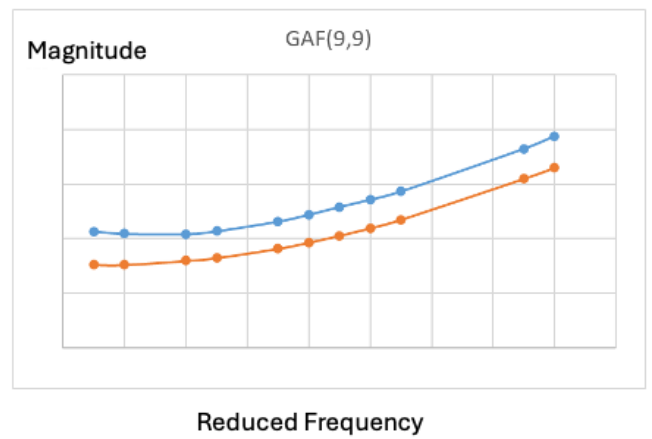
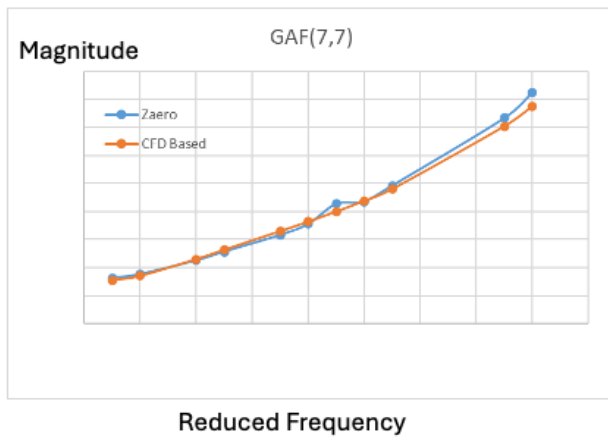


Figure 13. Comparison of ZAERO and LFD generalized aerodynamic forces for $M=1.05$, diagonal components for flexible modes 7 and 9.

V. Conclusions

The full paper will present linear and nonlinear (CFD-based) aeroelastic results at several Mach numbers and dynamic pressures that are aligned with flight conditions for the envelope expansion mission. Results to be presented include time-domain FUN3D aeroelastic analyses, including generalized coordinates to demonstrate stability at those conditions. Results from AEROM applications will include comparison of generalized coordinates and generalized aerodynamic forces (GAFs) with FUN3D solutions as well as aeroelastic dynamic pressure root locus plots for each Mach number. Results from the LFD method will include comparison of GAFs with ZAERO as well as V-g-f plots for both ZAERO and LFD.

References

- ¹Anderson, W. K., Biedron, R. T., Carlson, J.-R., Derlaga, J. M., Diskin, B., Druyor, C. T., Gnoffo, P. A., Hammond, D. P., Jacobson, K. E., Jones, W. T., Kleb, B., Lee-Rausch, E. M., Liu, Y., Lohry, M. W., Nastac, G. C., Nielsen, E. J., Padway, E. M., Park, M. A., Rumsey, C. L., Thomas, J. L., Thompson, K. B., Walden, A. C., Wang, L., Wood, S. L., Wood, W. A., and Zhang, X., "FUN3D 14.2 Manual," Tech. Rep. TM-20250002308, NASA, April 2025.
- ²Anderson, W. K. and Bonhaus, D. L., "An Implicit Upwind Algorithm for Computing Turbulent Flows on Unstructured Grids," *Computers & Fluids*, Vol. 23, No. 1, 1994, pp. 1–21.
- ³Biedron, R. T. and Thomas, J. L., "Recent Enhancements to the FUN3D Flow Solver for Moving-Mesh Applications," *AIAA 47th Aerospace Sciences Meeting*, Orlando, Florida, January 5–8 2009.
- ⁴Anderson, W. K., Newman, J. C., and Karman, S. L., "Stabilized Finite Elements in FUN3D," *55th AIAA Aerospace Sciences Meeting*, 2017.
- ⁵Jacobson, K. E., Stanford, B. K., Wood, S. L., and Anderson, W. K., "Flutter Analysis with Stabilized Finite Elements based on the Linearized Frequency-domain Approach," *58th AIAA Aerospace Sciences Meeting*, Orlando, Florida, January 6–10 2020.
- ⁶Spalart, P. and Allmaras, S. R., "A One-Equation Turbulence Model for Aerodynamic Flows," *Recherche Aeronautique*, Vol. 1, 1994, pp. 5–21.
- ⁷Allmaras, S. R., Johnson, F. T., and Spalart, P. R., "Modifications and Clarifications for the Implementation of the Spalart-Allmaras Turbulence Model," 2012.
- ⁸Juang, J.-N. and Pappa, R. S., "An Eigensystem Realization Algorithm for Modal Parameter Identification and Model Reduction," *Journal of Guidance, Control, and Dynamics*, Vol. 8, 1985, pp. 620–627.
- ⁹Juang, J.-N., Phan, M., Horta, L. G., and Longman, R. W., "Identification of Observer/Kalman Filter Markov Parameters: Theory and Experiments," *Journal of Guidance, Control, and Dynamics*, Vol. 16, 1993, pp. 320–329.
- ¹⁰Silva, W. A., "AEROM: NASA's Unsteady Aerodynamic and Aeroelastic Reduced-Order Modeling Software," *Aerospace*, Vol. 5(2), No. 41, 2018.